

DeepStroke: An Efficient Stroke Screening Framework for Emergency Rooms with Multimodal Adversarial Deep Learning

Tongan Cai^{a,*}, Haomiao Ni^{a,*}, Mingli Yu^a, Xiaolei Huang^a, Kelvin Wong^b, John Volpi^c, James Z. Wang^a, Stephen T.C. Wong^b

^aCollege of Information Sciences and Technology, The Pennsylvania State University, University Park, Pennsylvania 16803, USA

^bT.T. and W.F. Chao Center for BRAIN & Houston Methodist Cancer Center, Houston Methodist Hospital, Houston, Texas 77030, USA

^cEddy Scurlock Comprehensive Stroke Center, Department of Neurology, Houston Methodist Hospital, Houston, Texas 77030, USA

ARTICLE INFO

Article history:

Communicated by ?

2000 MSC: 68T10, 68T45, 92C55

Keywords: Stroke, Multi-Modal, Computer Vision

ABSTRACT

In an emergency room (ER) setting, the diagnosis of stroke is a common challenge. Due to excessive execution time and cost, an MRI scan is usually not available in the ER. Clinical tests are commonly referred to in stroke screening, but neurologists may not be immediately available. We propose a novel multimodal deep learning framework, *DeepStroke*, to achieve computer-aided stroke presence assessment by recognizing the patterns of facial motion incoordination and speech inability for patients with suspicion of stroke in an acute setting. Our proposed *DeepStroke* takes video data for local facial paralysis detection and audio data for global speech disorder analysis. It further leverages a multi-modal lateral fusion to combine the low- and high-level features and provides mutual regularization for joint training. A novel adversarial training loss is also introduced to obtain identity-independent and stroke-discriminative features. Experiments on our video-audio dataset with actual ER patients show that the proposed approach outperforms state-of-the-art models and achieves better performance than ER doctors, attaining a 6.60% higher sensitivity and maintaining 4.62% higher accuracy when specificity is aligned. Meanwhile, each assessment can be completed in less than 6 minutes, demonstrating the framework's great potential of clinical implementation.

© 2021 Elsevier B. V. All rights reserved.

1. Introduction

Stroke is a common cerebrovascular disease that can cause lasting brain damage, long-term disability, or even death (Centers for Disease Control and Prevention, 2005). It is the second leading cause of death and the third leading cause of disability worldwide (Johnson et al., 2016). According to the Centers for Disease Control and Prevention (2020), someone in the United States has a stroke every forty seconds and someone dies of a stroke every four minutes. In acute ischemic stroke where brain

tissue lacks blood supply, the shortage of oxygen needed for cellular metabolism quickly causes long-lasting tissue damage. If identified and treated in time, many interventions are available and an acute ischemic stroke patient will have a greater chance of survival and subsequently a better quality of life.

However, delays related to misdiagnosis and underdiagnosis are common and limit treatment options are inevitable during the presentation, evaluation, diagnosis, and treatment of stroke (Rafay et al., 2009). Other than clinical judgment, there is no point-of-care test to reliably and rapidly diagnose acute ischemic stroke. Currently, the gold standard test for stroke is advanced neuro-imaging including diffusion-weighted MRI scan (DWI) that detects brain infarct with high sensitivity and specificity. Although accurate, DWI is usually not accessible in the emergency room (ER) due to limited equipment availabil-

*T. Cai and H. Ni made equal contributions. All correspondence should be addressed to T. Cai, J.Z. Wang, and S.T.C. Wong.

e-mail: cta@psu.edu (Tongan Cai), jwang@psu.edu (James Z. Wang), stwong@houstonmethodist.org (Stephen T.C. Wong)

ity and high operating cost. Even in advanced centers with ER availability of MRI, the turn around time for patient transport, testing, and results adds 30-60 minutes. Therefore, in the actual ER scenario, clinicians commonly adopt the following three tests: the Cincinnati Pre-hospital Stroke Scale (CPSS) (Kothari et al., 1999), the Face Arm Speech Test (FAST) (Harbison et al., 2003), and the National Institutes of Health Stroke Scale (NIHSS) (NIH, 2003). All these methods assess the presence of any unilateral facial droop, arm drift, and speech disorder. The patient is requested to repeat a specific sentence (CPSS) or have a conversation with the doctor (FAST), and abnormalities arise when the patient slurs, fails to organize his speech, or is unable to speak. For NIHSS, face and limb palsy conditions are also evaluated. However, the scarcity of neurologists (Leira et al., 2013) makes such tests difficult to be timely and effectively conducted in all stroke emergencies. The evaluation may also fail to detect stroke cases where only very subtle facial motion deficits exist—that clinicians are unable to observe.

Recently, with the help of machine intelligence, researchers have proposed more and more accurate detection and evaluation methods for neurological disorders. Besides working on computer-aided medical image understanding for CT and MRI images (Xue et al., 2018; Yao et al., 2018; Akkus et al., 2017), many researchers are now focusing on alternative contactless, efficient, and economic ways for the analysis of various neurological conditions. One of the most popular domains is the detection of facial paralysis with computer vision, *i.e.*, letting machines detect the anomalies in the subjects’ faces. However, the majority of work neglects the readily available and indicative speech audio features (Thevenot et al., 2017), which can be an important source of information in stroke diagnosis. Also, current methods ignore the spatiotemporal continuity of facial motions (He et al., 2008; Hakata et al., 2013; Flores-Mondragón et al., 2015) and fail to tackle the problem of static/natural asymmetry. Common video classification frameworks like I3D (Carreira and Zisserman, 2017) and SlowFast (Feichtenhofer et al., 2019) also fail to serve the stroke pattern recognition purpose due to the lack of training data and quick overfitting as “subject-remembering” effect.

Moreover, few datasets of high quality have been constructed in stroke diagnosis domain. The current clinical datasets (Perveen, 2019; Kihara et al., 2011; Hsu et al., 2018; Greene et al., 2019) are small (with hundreds of images or dozens of videos) and unable to comprehensively represent the diversity in stroke patients in terms of gender, race/ethnicity, and age. Also, they either evaluate between normal subjects versus those with clear signs of a stroke (Bandini et al., 2016; Ngo et al., 2016) or deal with full synthetic data (*i.e.*, healthy people pretend to have palsy facial patterns) (Zhuang et al., 2018; Storey and Jiang, 2018); some others establish experimental settings with hard constraints on the patient’s head (Bevilacqua et al., 2011; Hamm et al., 2011; Wang et al., 2014)—all of which will hinder their clinical implementation for ER screening or patient self-assessment.

In this paper, we propose a novel deep learning framework, named *DeepStroke*, to accurately and efficiently analyze the presence of stroke in patients with suspicion of a stroke. The

problem is formulated as a binary classification task, *i.e.*, stroke vs. non-stroke. Instead of taking a single-modality input, the core network in *DeepStroke* consists of two temporal-aware branches, the video branch for local facial motion analysis and the audio branch for global vocal speech analysis, to collaboratively detect the presence of stroke patterns. A novel lateral connection scheme between these two branches is introduced to combine the low- and high-level features and provide mutual regularization for joint training. To mitigate the “subject-remembering” effect, *DeepStroke* also makes use of adversarial learning to learn subject-independent and stroke-discriminative features for the network.

To evaluate our proposed *DeepStroke*, we construct a stroke patient video/audio dataset that records the facial motions of the patients during their process of performing a set of vocal speech tests when they visit the ER. The recruited participants are all showing some level of neurological conditions with a high risk of stroke when visiting the ER, which is closer to the real ER scenarios and much more challenging than distinguishing stroke patients from healthy people. Our dataset includes diverse patients of different genders, races/ethnicity, ages, and at different levels of stroke conditions; the subjects are free of motion constraints and are in arbitrary body positions, illumination conditions, and background scenarios, which can be regarded as “in-the-wild.” Experiments on our dataset show that the proposed *DeepStroke* framework can achieve high performance and even outperform trained ER clinicians for stroke diagnosis while maintaining a manageable computation workload.

A preliminary version of this work was presented in our earlier publication (Yu et al., 2020). In this paper, we substantially extend our prior work in the following aspects: (1) We substitute the text transcript inputs with the spectrogram input and replace the text LSTM with ResNet-18 to maintain the most of speech information, reduce errors induced by the transcription process as well as ease the later feature fusion with video module. (2) We introduce a lateral connection to the two branches to resolve unstable convergence of network caused by different training dynamics of branches and share low-level/high-level features for a better combination of the global context (audio) and local representation (video). (3) We introduce adversarial training scheme aiming to remove the subject identity features from the input to alleviate the “subject-remembering” effect of the deep neural networks. (4) We significantly enlarge the dataset with newly collected data to support extensive new experiments on our proposed new framework.

The **main contributions** of this work are summarized below.

1. We constructed a real ER patient facial video and vocal audio dataset for stroke screening with diverse participants. The videos are collected “in-the-wild,” with unconstrained patient body positions, environment illumination conditions, and background scenarios.
2. We propose a deep-learning multimodal framework, *DeepStroke*, that highlights its video-audio multi-level feature fusion scheme that combines global context to local representation, the adversarial training that extracts identity-independent stroke features, and the spatiotemporal pro-

positional mechanism for frontal human facial motion sequences.

3. The proposed multi-modal method achieves high diagnostic performance and efficiency on our proposed challenging dataset and outperforms the clinicians, demonstrating its high clinical value to be deployed for real ER use.

2. Related Works

2.1. Facial motion analysis for medical diagnosis

In the past two decades, researchers have been striving for more and more novel facial motion analysis methods to achieve accurate detection and evaluation of facial paralysis and other medical conditions. Many early works focused on static image analysis. Rogers *et al.* (2007) aimed to detect the improvement in abnormal facial movements after treatment with botulinum toxin A; Dong *et al.* (2008) introduced a “face nerve index” based on coordinates of image feature points and achieved an accurate classification of facial paralysis levels. Some others utilized multiple images in a sequence for improved analysis, like He *et al.* (2007) and Green and Guan (2004). With video data, researchers can capture between-frame motions of patient faces and temporal patterns in facial abnormalities. For example, Frey *et al.* (2008) analyzed the video trajectories of facial regions for face paralysis detection and evaluation; Bandini *et al.* (2017) extracted articulatory movements of patient faces in a video to identify patterns of Parkinson’s disease. A small video dataset for facial paralysis has been offered by Greene *et al.* (2019) along with the eFACE (Banks *et al.*, 2015), House-Brackmann (House and Brackmann, 1985), and Sunnybrook (Ross *et al.*, 1996) metrics. There is not any publicly-available image or video database specifically designed for the evaluation of stroke within a patient due to the concern of personal identity leakage and IRB constraints; if no real patient case is available, researchers will have to use synthetic datasets like CK+ (Lucey *et al.*, 2010) where only healthy participants are involved. Also, biases in genders, ages, and races will arise as the majority of the prior datasets only have a limited number of subjects.

With recent developments in computer vision and especially face alignment, facial landmark is becoming a popular representation of facial patterns. Anping *et al.* (2017) measured asymmetry for facial movement images based on facial landmarks; Zhuang *et al.* (2018) and Szczapa *et al.* (2019) also introduced similar facial landmark-based methods on video or image data. Wang *et al.* (2016) and Zhuang *et al.* (2019) stratified the face of a patient into multiple regions and considered regional information with landmarks. While easy to obtain, the landmarks are not robust and suffer greatly from illumination, occlusion, and motion. Some more recent works design deep learning methods for the task. Song *et al.* (2018) develops an Inception-DeepID-FNP neural network for paralysis classification, Storey and Jiang (2018) considers a multi-task network for both face detection and facial asymmetry evaluation, and Guo *et al.* (2017) introduces a deep learning framework to classify facial paralysis with regard to the H-B standard. However, all these deep learning frameworks suffer from bad head poses,

non-facial motions. To address the alignment issues, the majority of prior works set up experimental settings with uniform illuminations and put up hard constraints on the subjects’ heads to avoid alignment issues. Such simplification of scenarios greatly hinders the clinical value of these proposed methods.

Upon reviewing the above literature, we concluded that existing approaches either evaluate their methods between subjects that are normal versus those with clear signs of a stroke, deal with only synthetic data, fail in capturing the spatiotemporal details of facial muscular motions, or rely on experimental settings with hard constraints. Without considering challenges in real emergencies such as illumination variations, pose changes, skin color, and subtleties of patterns, such methods are not practical in real clinical practice or for patient self-assessment.

2.2. Disentangle representation learning

Our work is also closely related to disentangle representation learning. Tran *et al.* (2017) proposed DR-GAN to learn a generative and discriminative representation for pose-invariant face recognition. Liu *et al.* (2018) proposed the D^2AE framework to adversarially learn the identity-independent features for identity verification and the identity-dispelled features to fool the verification system. Zhang *et al.* (2019) proposed an AutoEncoder framework to explicitly disentangle pose and appearance features from RGB imagery and the LSTM-based integration of pose features over time produces the gait feature. Lu *et al.* (2019) proposed an unsupervised domain-specific image deblurring framework by disentangling the content and blur features. Lee *et al.* (2018) proposed an image-to-image translation framework by disentangling image features into a domain-invariant content space and a domain-specific attribute space and combining them to produce diverse output.

Especially, learning subject-independent stroke patterns for diagnosis is a similar process as extracting identity-independent features for facial expression recognition (FER), which also aims to detect patterns of facial movements. Meng *et al.* (2017) designed identity-contrasting loss that goes in parallel with the expression-related loss to achieve identity-invariant expression recognition. Cai *et al.* (2019) proposed a conditional generative model to transform an average neutral face into an average expressive face with the same expression as the input image that is naturally identity-independent. Wang *et al.* (2019) constructed a pose discriminator and a subject discriminator to classify the pose and the subject from the extracted feature representations, respectively, to make them robust to poses and subjects. In this work, we adopt a similar approach and set up identity-related discriminators, and use an adversarial training scheme to extract identity-independent features. To our knowledge, our work is the first attempt that introduces adversarial training loss to stroke diagnosis tasks.

2.3. Multimodal deep learning

Deep networks that learn features over multiple modalities via shared representation learning (Ngiam *et al.*, 2011) have achieved outstanding performance on various multimedia tasks. Intuitively, when more than one form of data is available, a

deep network that utilizes most of them and takes aligned information from different sources, where each modality tends to complement each other and incorporate richer information, will usually result in higher task performance than using each information source individually. The idea of multimodal deep learning has been making great improvements to domains including emotion recognition (Kahou *et al.*, 2016), disease diagnosis (Xu *et al.*, 2016), object detection (Eitel *et al.*, 2015), etc. Common modalities include text, audio, vision and they can complement each other within a multi-modal deep neural network.

Specifically for disease diagnosis, multimodal methods have been proven useful to integrate patient data from multiple platforms or in different forms. Li and Shen (2018) proposed a multi-view deep learning framework (MvNet) with three branches to segment multimodal brain images from different view-points, *i.e.* slices along x -, y -, z -axes; Menegotto *et al.* (2020) developed a multimodal deep machine learning architecture for hepatocarcinoma diagnosis with computed tomography images, laboratory test results, anthropometric and sociodemographic data as input; to model the difficulties to start or to stop movements for patients with Parkinson’s disease, Vásquez-Correa *et al.* (2019) conducted multimodal deep learning over information from speech, handwriting, and gait; Liang *et al.* (2015) proposed multimodal deep belief network (DBN) to cluster cancer patients observation data from different platforms. The fusion of medical imaging and electronic health records using deep learning has been another heated topic of these years (Huang *et al.*, 2020), which will make pixel-based models and contextual data from electronic health records (EHR) work cooperatively for the diagnostic purpose.

Stroke diagnosis can also benefit from multimodal deep learning. To diagnose a stroke case, neurologists detect the facial deficits on the patient’s face or the inability in speech—the two modalities tend to work jointly. In this work, we adopt the multimodal idea to allow the facial video and vocal audio to work together for a final diagnosis.

3. Dataset

The clinical dataset for this study was acquired in the ERs of the Houston Methodist Hospital by the physicians and caregivers from the Eddy Scurlock Stroke Center at the Hospital under an IRB-approved study.¹ It has taken more than a year for us to recruit a large pool of patients in various stroke-related emergencies, and the cohort is still expanding. The subjects chosen are patients with suspicion of stroke or have already been identified with a high risk of stroke (transferred from other health providers) while visiting the ER. To help preserve the patients’ personal information, we only transmitted limited information that we think is sufficient for this study between institutes to avoid any identifiable information to be collected and dispensed. The patients are only assessed when they’re in a relatively stable condition so the collection of data will not impose extra risk to very emergency cases. Note that the gender ratio of

our dataset is relatively balanced without intervention, and the race/ethnicity or age distributions are not manually controlled, which would roughly represent the real distribution of the incoming ER patients. Potential bias will be discussed in Sec. 5.

Clinically, the ability of speech is an important and efficient indicator for the presence of stroke and is the preferable measurement doctors will use to make initial clinical impressions; if a potential patient slurs, mumbles, or even fails to speak, he or she will have a very high chance of stroke (Harbison *et al.*, 2003; Kothari *et al.*, 1999). During the evaluation and recording stage, we follow the NIH Stroke Scale (2003) and perform the following speech tasks on each subject: (1) to repeat the sentence “it is nice to see people from my hometown,” and (2) to describe a “cookie theft” picture as shown in Figure. 1a. The “cookie theft” task requires the subject to retrieve, think, organize, and express the information, which will end up evaluating the patient’s speech ability from both motor and cognitive aspects. It has been making great success in identifying patients with Alzheimer’s-related dementia, aphasia, and some other cognitive-communication impairments (Giles *et al.*, 1996), and would be suitable for our stroke screening purpose.



(a) The “Cookie Theft Picture”



(b) The setup of recording protocol.

Fig. 1: The speech task and the recording protocol.

The subjects are video recorded when they are performing the two tasks. The collection protocol is set up with an Apple iPhone X, as shown in Figure 1b. Note that a phone rack and an auxiliary microphone will be used if the patient is too weak to hold the device stably. Each video is accompanied by meta-data information on both clinical impressions by the ER physician (indicating the doctor’s initial judgment on whether the patient has a stroke or not from his/her speech and facial muscular

¹Houston Methodist IRB protocol No. Pro00020577, Penn State IRB site No. SITE00000562.

conditions) and ground truth from the diffusion-weighted MRI (including the presence of acute ischemic stroke, transient ischemic attack (TIA), etc.). Samples of such metadata information are shown in Table 1.

Table 1: Metadata info for subjects enrolled. (PE: Patient example)

PE	Complaint	Clinical Impression	Discharge Diagnoses	Details
1	Weakness	DR: Stroke / TIA	1, Acute ischemic stroke 2, Dyslipidemia 3, Type 2 diabetes A1c	L cortical infarct (precentral gyrus) and additional R corpus callosum (subacute)
2	Other - Neurologic problem	DR: Stroke / TIA	1, TIA 2, possible TIA versus seizure 3, acute metabolic encephalopathy 4, UTI 5, Obesity 6, HLD 7, HTN 8, Pre-diabetes 9, Hypertensive urgency 10, transient alteration of awareness	right vertebral artery, V3, V4 Unable to obtain MRI due to metal artifact
3	Tremor, Stuttering	Aphasia, Ataxia, Unspecified Tremor, CVA	1, Tremors	Neurology gave pt DDx of acute ischemic stroke, TIA, and toxic-metabolic. Workup ruled out CVA and indicated breakthrough seizure
4

We have been recruiting new subjects to expand the dataset. Up to the time of completing the manuscript, 79 males and 72 females have been recruited, non-specific of age, race/ethnicity, or the seriousness of stroke. Among the 151 individuals, 106 are patients diagnosed with stroke using MRI, 45 are patients who do not have a stroke but are diagnosed with other clinical conditions. A summary of demographics information is shown in Table 2. In this work, we formulate the diagnosing process as a binary classification task and only attempt to identify stroke/TIA cases from non-stroke cases. Though there are varieties of stroke subtypes, binary output has been sufficient to work as the screening decision in ER.

Table 2: Summary of subjects’ demographic information in the dataset.

Attribute	Group	Stroke	Non-Stroke	Total
Gender	Male	54	25	79
	Female	52	20	72
Age	≤ 65 y/o	60	24	84
	≥ 65 y/o	46	21	67
Ethnicity	Hispanic	7	4	11
	Non-Hispanic	95	39	134
	Opt-out	4	2	6
Race	African-American	34	9	43
	Other	72	36	108
All subjects		106	45	151

Our dataset is unique, as compared to existing ones (Guo *et al.*, 2017; He *et al.*, 2007), because our cohort consists of actual patients visiting the ERs and the videos are collected under unconstrained, or “in-the-wild” conditions. Existing work generally setup experimental settings before collecting the image or video data, which will result in uniform illumination conditions and minimum background noise. In our dataset, the patients can be in bed, sitting, or standing, where the background and illumination are usually not under ideal control conditions. Furthermore, a lot of previous works will enforce rigid constraints over

the subjects’ head motions, which avoids the alignment challenges and assumes stable face poses. We only asked patients to focus on the instructions, without rigidly restricting their motions, but using video processing methods to accommodate for the “in-the-wild” conditions. The acquisition of facial data in natural settings allows comprehensive evaluation of the robustness and practicability of our work for real-world clinical use, remote diagnosis, and self-assessment in most settings.

4. Methods

Fig. 2 shows the training framework of *DeepStroke*. We first preprocess the i -th input raw video to obtain the facial-motion-only, near-frontal face sequence \mathcal{X}_i and its corresponding audio spectrogram \mathcal{M}_i . Then we extract the audio-visual feature e_i from \mathcal{X}_i and \mathcal{M}_i by a lateral-connected dual-branch Encoder E , which includes a video module Γ_v for local visual pattern recognition, and an audio module Γ_a for global audio feature analysis. A subject Discriminator D is also employed to help E learn features that are insensitive to subject identity difference whereas sensitive to distinguish stroke from non-stroke. When training, we use the case-level label as a pseudo label for each video frame and train the *DeepStroke* network as a frame-level binary classification model. We also sample the intermediate output feature maps from different videos to train D and E adversarially. During inference, we first perform frame-level classification, and then calculate the case-level predictions by averaging over all frames’ probabilities to mitigate frame-level prediction noise. More details are described as follows.

4.1. Data Preprocessing

For each raw video, we propose a spatiotemporal proposal mechanism to extract frontal-face sequences from the raw video. For each audio extracted from the raw video, we transform the soundtrack to a spectrogram that represents the amplitude at each frequency level over time.

Spatiotemporal proposal of facial action video: In facial motion analysis, one challenge is to achieve good face alignment. As our data tend to be more “in-the-wild”, we introduce a pipeline to extract frame sequences with near-frontal facial pose and minimum non-facial motions. First, we detect and track the patient’s face with a rigid, square bounding box and estimate the poses. Frame sequences 1) estimated with significant roll, yaw, or pitch, 2) showing continuously changing pose metrics, or 3) having excessive head translation or too little change estimated with optical flow magnitude with the previous frame, are excluded (detailed criteria is presented in Section 5.1). A video stabilizer with a sliding window over the trajectory of between-frame affine transformations smooths out pixel-level vibrations on the sequences before they are passed to the Encoder E .

Speech spectrum analysis: Instead of transcribing the vocal audio to text corpus (Yu *et al.*, 2020), which may suffer from translation errors, we turned to spectrograms for speech analysis due to the following reasons: (1) Spectrogram is the complete representation of an audio file since the amplitude over frequency bands are captured over time. Recent deep learning-based transcription models commonly transform soundtracks

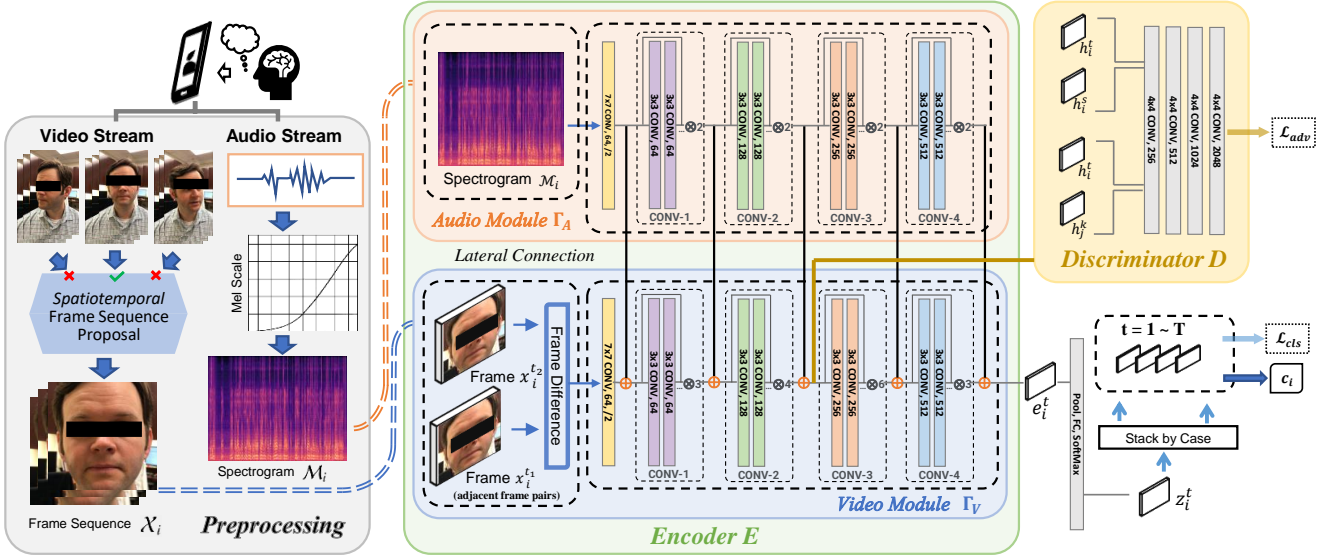


Fig. 2: The training framework of *DeepStroke*. The preprocessing part involves a spatiotemporal facial frame sequence proposal and a transformation of audio feature to spectrograms. In the encoder E , at any timestamp t , the input frame pairs x_i^1 and x_i^2 are guaranteed to be adjacent pairs, and the total spectrogram is duplicated and appended as the audio features for time t . The symbol \oplus indicates the concatenation with the lateral connection.

into spectrograms for their classification models (Hannun et al., 2014; Amodei et al., 2016). (2) By choosing spectrogram, which is image-like input, we can adapt similar networks for the two branches and ensure they have rather similar training dynamics to converge at a similar pace, which will make them cooperate better. In this work, we use the Mel Scale (Stevens et al., 1937) and Fast Fourier Transform (FFT) to transform the audio signal before plotting the spectrogram.

4.2. Model Design

As Fig. 2 shows, after preprocessing the raw input videos, we further extract stroke-discriminative and identity-independent features from the input video and audio via the feature encoder E and the subject discriminator D .

Feature Encoder. Let $X_i = (x_i^1, \dots, x_i^T)$ denotes a sequence of T temporally-ordered frames from the i -th input video and its corresponding spectrogram is M_i . We extract their features through feature encoder E , which includes one video module Γ_v and one audio module Γ_a , fused by lateral connection.

► *Video Module.* To extract temporal visual feature from the input X_i , a pair of adjacent frames from X_i is forwarded to the video module Γ_v . Due to the frame-proposal process, the original frame sequence sometimes has long gaps between two nearby frames, which will result in large, non-facial differences being captured. We tackle this by keeping track of frame index and only sample a specific number of real adjacent frame pairs in X_i (frame x_i^1 and x_i^2) to extract local visual information. Instead of directly inputting a pair of frames, for better capturing subtle facial motions between adjacent frames, we compute the image difference between x_i^1 and x_i^2 and then pass it through the network as the feature for the frame pair x_i^t .

► *Audio Module.* To extract disease patterns from the input audio spectrogram M_i , we feed M_i to the audio module Γ_a . Since M_i contains the whole temporal dynamics of input audio sequence, we append M_i to each frame pair x_i^t and x_i^{t+1} to

provide global context for the frame-level stroke classification.

► *Lateral Connection.* To effectively combine features of video X_i and audio M_i at different levels, we also introduce lateral connection (Xiao et al., 2020) between the convolutional blocks of the video module Γ_v and the audio module Γ_a . To ensure the features are aligned when being appended, we perform 1×1 convolution (Lin et al., 2013) to project the global audio feature to the same embedding space as the local frame features and then sum them up. Compared with the late fusion of two branches used in our prior work (Yu et al., 2020), lateral connections-based fusion not only combines more levels of features, but also enables different branch dynamics to stay similar, which will maintain the convergence rate of each branch to be relatively closer and help the global context better complement the local context during the training stage. The final fused features e_i^t are passed through the fully-connected and softmax layers to generate the frame-level class probability score z_i^t . The case-level prediction c_i is then obtained by stacking and averaging the frame-level predictions.

Subject Discriminator. Due to the relatively small number of available videos, it is easy and tempting for the encoder E to memorize the facial and audio features of each subject and just match testing subjects with training subjects based on similarity in appearance and voice when performing the inference. To avoid this issue of classification based on subject-dependent features, we further design a subject discriminator D to help encoder E learn subject-independent features. The discriminator D is designed to simply distinguish whether the input pair of intermediate features from Encoder E are from the same subject or not and will be used to adversarially train the encoder E .

In theory, the network of *DeepStroke* can employ various networks as its backbone. Here we choose ResNet-34 for Γ_v and ResNet-18 for Γ_a to accommodate for the relatively small size of video dataset, the simplicity of the spectrogram, and reduce the computational cost of the framework. For the discrimina-

tor D , we simply follow the design of DCGAN (Radford et al., 2015) with 4 convolution layers and binary output. For the intermediate feature input to the discriminator, we take the output feature from the second block (CONV-2) of the ResNet-34 after the lateral connection at this level. The choice of intermediate feature is ablated in section 5.3.1.

4.3. Model Training and Testing

We employ the following loss functions to train *DeepStroke*.

Classification loss: To help E learn stroke-discriminative features, we use a standard binary cross-entropy loss between the prediction z_i^t and video label \mathcal{Y}_i for all the training videos and their T frames:

$$\mathcal{L}_{\text{cls}}(E) = - \sum_i \sum_t (\mathcal{Y}_i \log z_i^t + (1 - \mathcal{Y}_i)(1 - \log z_i^t)) . \quad (1)$$

Adversarial loss: To encourage Encoder E to learn subject-independent features, we introduce a novel adversarial loss to ensure that the output feature map h_i^t does not carry any subject-related information. We impose this via an adversarial framework between the subject discriminator D and feature encoder E , as shown in Fig. 2. The latter E will provide a pair of feature maps, either computed from the same subject video (h_i^t, h_i^s) at time t and s , or from different subject videos (h_i^t, h_j^k) at time t and k , where time s and k can be randomly chosen. Discriminator D then attempts to classify the pair as being from the same/different subject video using a l_2 loss, as LS-GAN (Mao et al., 2017) adopts:

$$\mathcal{L}_{\text{adv}}(D) = - \sum_i \sum_t (\|D(h_i^t, h_i^s)\|_2 + \|1 - D(h_i^t, h_j^k)\|_2) , \quad (2)$$

The adversarial framework further imposes a loss function on the feature encoder E that tries to maximize the uncertainty of the discriminator D output on the pair of frames:

$$\mathcal{L}_{\text{adv}}(E) = - \sum_i \sum_t \left(\left\| \frac{1}{2} - D(h_i^t, h_i^s) \right\|_2 + \left\| \frac{1}{2} - D(h_i^t, h_j^k) \right\|_2 \right) , \quad (3)$$

Thus the encoder E is encouraged to produce features that the discriminator D is unable to classify if they come from the same subject or not. In so doing, the features h cannot carry information about subject identity, thus avoiding the model to perform inference based on subject-dependent appearance/voice features. Note that our model is different from classic adversarial training used in GANs (Goodfellow et al., 2014) since we only focus on classification and there is no generator network in our framework.

Overall training objective: During training, we minimize the sum of the above losses:

$$l = \mathcal{L}_{\text{cls}}(E) + \lambda(\mathcal{L}_{\text{adv}}(E) + \mathcal{L}_{\text{adv}}(D)) , \quad (4)$$

where λ is the balancing parameter. The first two terms can be jointly optimized, but the discriminator D is updated while the encoder E is held constant.

When testing, because our model is trained with pseudo frame-level labels, to mitigate frame-level prediction noise, we first perform frame-level classification using encoder E , and then we calculate the case-level prediction by summing and normalizing class probabilities over all frames, and the predicted case label will be the class with higher probability.

5. Experiment

To better present the details of our proposed method, we first introduce the setup and implementation details and then show the comparative study with baselines. We also ablate the power of model components and structures to validate our design.

5.1. Setup and implementation

The whole framework² is running on Python 3.7 with Pytorch 1.1, OpenCV 3.4, CUDA 9.0, and Dlib 19. Both ResNet models are pre-trained on ImageNet (Deng et al., 2009). Each .mov file from the iPhone will first be separated as frame sequences as batches of .png files and one global .wav audio file.

For the frame sequences, we detect the location of the patient’s face as a square bounding box with Dlib’s face detector (King, 2009) and track it using the Python implementation of ECO tracker (Danelljan et al., 2017). We perform pose estimation by solving a direct linear transformation from the 2D landmarks predicted by Dlib to a 3D ground truth facial landmarks of an average face, which resulted in three values corresponding to the angular magnitudes over three axes (pitch, roll, yaw). To tolerate estimation errors, we regard those with angular motions less than a threshold β_1 as frontal faces. A 5-frame sliding window records the between-frame changes (three differences) in the pose. If the total changes (3 axes) sum up to more than a threshold β_2 , we abandon the frames starting from the first position of the sliding window. In the meantime, the between-frame changes are measured by optical flow magnitude. If the total estimated change is smaller than β_l (no motion) or larger than β_h (non-facial motions), we also exclude the frame. We empirically set $\beta_1 = 5^\circ$, $\beta_2 = 20^\circ$, $\beta_l = 0.01$ and $\beta_h = 150$. After manipulation, we crop the size of each frame in the videos to $224 \times 224 \times 3$ to align with the ImageNet dataset. The real frame numbers are also kept to ensure that only adjacent frame pairs are loaded to the network.

For the audio files, we load and trim using *librosa*, and plot the Log-Mel spectrogram, where the horizontal axis is the temporal line, the vertical axis is the frequency bands, and each pixel shows the amplitude of the soundwave at the specific frequency and time. The output spectrogram is also set to the size of $224 \times 224 \times 3$.

The entire pipeline is trained on a personal computer with a quad-core CPU, 16GB RAM, and a NVIDIA GPU with 11GB VRAM. To accommodate for the class imbalance inside the dataset and ER setting, a higher class weight (2.0) is assigned to the non-stroke class. In evaluation, we refer to the accuracy, specificity, sensitivity, and area under the ROC curve (AUC) from 5-fold cross-validation results over the full dataset. The learning rate is tuned to $1e-5$ and we early stop at epoch 8 due to the quick convergence of the network. The batch size is set to be 64 and λ in (4) is set to be 10. The same parameters are also applied to the baselines and the ablation studies.

5.2. Baselines and comparison

We construct baseline models for both video and audio tasks. For each video/audio, the ground truth for comparison is the

²Codes will be publicly available after the acceptance of the manuscript.

Table 3: Comparative study results with baseline. Raw: results with threshold 0.5 after the final softmax output; aligned: results with the threshold that makes the specificity aligned. Best values are in bold.

Method \ Metrics	Accuracy (%)		Specificity (%)		Sensitivity (%)		AUC
	Raw	Aligned	Raw	Aligned	Raw	Aligned	
Module Γ_a (Audio)	60.93	46.36	22.22	53.33	77.36	43.40	0.5168
Module Γ_v (Video)	70.86	52.31	13.13	53.33	95.28	51.89	0.5381
I3D (Video)	62.25	42.38	15.55	53.33	82.08	37.73	0.4419
SlowFast (Video)	67.55	36.42	2.22	53.33	95.28	29.25	0.3981
MMDL (Audio + Video)	70.20	58.27	20.00	53.33	91.50	60.38	0.5893
DeepStroke (Audio + Video)	68.21	63.56	37.77	53.33	81.13	67.92	0.6631
Clinical Impression (CI)	58.94		53.33		61.32		0.5733

binary diagnosis result obtained through the MRI scan. Our chosen baselines are introduced as follows:

- **Audio Module Γ_a .** The first corresponding baseline is the strip audio module from the proposed method that takes the preprocessed spectrograms as input. We use the same setup to train the audio module and obtain binary classification results on the same data splits.
- **Video Module Γ_v .** The other baseline is the strip video module from the proposed method that takes the preprocessed frame sequences as input. We use the same adversarial training scheme to train the video module and obtain binary classification results on the same data splits.
- **I3D.** The Two-Stream Inflated 3D ConvNet (I3D) (Carreira and Zisserman, 2017) expands filters and pooling kernels of 2D image classification ConvNets into 3D to learn spatiotemporal features from videos. It was the state-of-the-art model years ago. For our task, I3D can be inferior due to the calculation of optical flow can be time-consuming and results in more noises.
- **SlowFast.** The SlowFast (Feichtenhofer et al., 2019) network is a video recognition network proposed by Facebook that involves (i) a Slow pathway to capture spatial semantics, and (ii) a Fast pathway to capture motion at fine temporal resolution. SlowFast achieves strong performance on action recognition in video and has been a powerful state-of-the-art model in recent years.
- **MMDL.** Our prior work MMDL (Yu et al., 2020) is a preliminary version of the proposed two-branch method that takes similar preprocessed frame sequences for the video branch, but text transcripts for the audio branch. The video branch uses feature difference instead of image difference (which we will ablate later), and the audio branch was an LSTM that performs text classification. Due to drastically different network structures, the two branches only have connections in the final layer using a “late-fusion” scheme.

Because our objective is to perform the stroke screening for incoming patients, the proposed methods and the baselines are compared to the ER doctors’ clinical impression we obtained

with the metadata information. We further examine the effectiveness of our proposed methods with clinical impression and baselines by aligning the specificity of each method to be the same through changing the threshold for binary cutoffs, while checking and comparing for other measurements. The results are shown in Table 3. For better comparison, the ROC curves for the proposed model and baselines are also plotted in Fig. 3, together with the clinical impression from the physicians.

From both Table 3 and Fig. 3, one can see that our proposed *DeepStroke* outperforms several state-of-the-art methods as well as its single module variants. Compared with our prior work MMDL, *DeepStroke* improves specificity by 17.77% and AUC by 0.0738. This is a major improvement considering the prior work has already demonstrated good performance on the preliminary version of the dataset. We believe the improvements came from the following aspects: i) firstly, by adopting a different audio representation and introducing the lateral connections, the proposed framework resolves the unstable convergence problem in the prior work caused by different training dynamics of branches, while also sharing low- and high-level features for a better combination of global audio context and local frame features; ii) secondly, our adversarial training scheme can keep the network from remembering the identity features and extract pure stroke-related features for the network to learn, which also mitigates the overfitting problem. The two aspects are discussed in the following ablation studies; iii) in another aspect, using spectrograms instead of the text transcripts will maximally preserve the patterns in the original audio files since the soundwave information is fully presented without inference, addition, or deletion.

Moreover, comparing the Video Module Γ_v with two state-of-the-art video recognition models, we can also see a much higher model performance. When specificity is aligned, Video Module Γ_v is achieving 9.93% higher accuracy, 14.16% higher sensitivity, and 0.0972 higher AUC than I3D and 15.89% higher accuracy, 22.64% higher sensitivity and 0.14 higher AUC than SlowFast. When compared with ER physicians, one can see that the proposed *DeepStroke* shows 0.0898 higher AUC value, and 6.6% higher sensitivity, and 4.62% higher accuracy when aligned the same specificity with clinicians, which illustrating its practicability and effectiveness.

Through the experiments, all the methods are experiencing

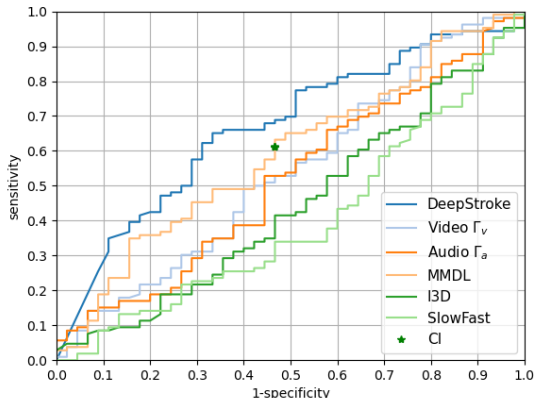


Fig. 3: The ROC curve from 5-fold cross-validation for the proposed *DeepStroke* and other baselines. The green dot shows the performance of clinical impression (CI) from ER physicians.

low specificity (*i.e.*, identifying non-stroke cases), which is reasonable because our subjects are patients with suspicion of stroke or showing neurological disease-related patterns, rather than the general public. The nature of our task is much harder than previous works.

With new patients continuously being added to the cohort, our dataset is becoming more and more diverse and even more challenging for the clinicians (for the original dataset, the performance of the clinicians was 72.94% accuracy, 77.78% specificity, 70.68% sensitivity, and 0.7423 AUC). We infer this is due to the addition of a decent number of hard cases, where the patterns for stroke are too subtle for the clinicians to capture. Even so, when we have aligned specificity, the proposed method still outperforms the clinicians. ER doctors tend to rely more on the speech abilities of the patients and may have difficulty in cases with too subtle facial motion incoordination. We infer that the video module in our framework can detect those subtle facial motions that doctors can neglect and complement the diagnosis based on speech/audio. The drop in the specificity is regarded as permissible comparing to the improvements in sensitivity, since in stroke screening, failing to spot a patient with stroke (false-negative) will end up with very serious results. On the other hand, when making the decisions, the ER doctors have access to emergency imaging reports and other information in the Electronic Health Records (EHR) besides the video and audio information.

5.3. Ablation study

5.3.1. Model designs

To evaluate the effectiveness of different designs in our proposed model, we perform the following ablation studies:

- **Late fusion only.** The lateral connection we designed for the two branches was updated from the late fusion scheme in our prior work to connect the two branches at different levels. An experiment was made to only use the late fusion as a comparison to the full proposed model to show the power of the lateral connection.

- **Model w/o adv.** The adversarial training scheme aims to extract stroke-related identity-independent features. We experiment on the same proposed model that was trained without the adversarial scheme to see the improvements.
- **Frame difference.** In the proposed method, we set the two consecutive frames to form a difference at the very beginning of the network, but such difference can be made elsewhere—in the middle of the network or at the back of the network (*i.e.*, the deep features generated from the framework). An extra experiments are conducted on a different frame difference scheme used in our prior work.
- **Discriminator feature input stage.** When adversarial training for distilling the subjects’ identities, our network takes the encoded features after two blocks of ResNet. We have other stages where features are extracted for the adversarial training, (*i.e.*, after the first block, after the third block, and right before the final fully-connected layer). We experiment on the full network with the only change to be the stage where we take out the encoded features.

Table 4: Ablation study results. The first entry ablates the lateral connection we designed over the late fusion scheme, the second entry ablates the adversarial training scheme, the third block ablates the other choices of making frame pair difference, and the third block ablates other choices of extracting encoded features for the discriminator.

Method \ Metrics	Accuracy (%)	Specificity (%)	Sensitivity (%)	AUC
Late Fusion	70.86	2.22	100	0.5779
w/o adv	68.87	17.78	90.57	0.5568
Conv-Diff	71.52	22.22	92.45	0.6486
Feature #1	72.84	26.66	92.45	0.5788
Feature #3	68.21	15.55	90.56	0.5910
Feature #4	68.87	6.66	95.28	0.5662
<i>DeepStroke</i> (Ours)	68.21	37.77	81.13	0.6631

From Table 4, we could conclude that both the lateral connection and the adversarial training have been improving the performance of the framework as expected. The lateral connection improves the overall statistics with 0.0852 in AUC, indicating a better learning outcome that may result from better balanced two-branch learning dynamics. The adversarial training drastically improved the specificity (19.99% as shown) and resulted in a better learning result (0.0971 improvements in AUC), and we believe the features for stroke are more clearly revealed with this training scheme.

5.3.2. Model fairness

We also examined the discrepancy between different genders, races/ethnicity, and age groups in our dataset. Specifically, we examine the following attribute groups in Table 5 and report the validation results within the 5-fold cross-validation experiment result on the proposed model:

- **Gender.** There have been studies pointing out that gender discrepancy is noticeable for stroke: women show unique patterns that are often neglected (Colsch and Lindseth,

Table 5: Validation results for different attribute groups. The number in the bracket indicates the total number of cases in the group. Notice that some subjects opt out for ethnicity or race questions and are excluded. Model: Our Proposed *DeepStroke*, CI: Clinical Impression. Values in red are considered to yield fairness concerns.

Group	Attr.	Metrics		Accuracy (%)		Specificity (%)		Sensitivity (%)		AUC	
		Model	CI	Model	CI	Model	CI	Model	CI	Model	CI
Gender	Male (79)	62.03	58.22	28.00	46.15	77.78	64.15	0.6204	0.5515		
	Female (72)	75.00	59.72	50.00	63.15	84.62	58.49	0.7255	0.6082		
Age	≤ 65 y/o (84)	73.81	61.90	54.17	62.96	81.67	61.40	0.7069	0.6218		
	≥ 65 y/o (67)	61.19	55.22	19.05	38.89	80.43	61.22	0.6542	0.5006		
Ethnicity	Hispanic (11)	81.81	72.72	50.00	33.33	100.00	87.50	0.8214	0.6042		
	Non-Hispanic (134)	67.16	58.20	35.90	53.66	80.00	60.21	0.6502	0.5693		
Race	African American (43)	65.11	53.49	11.11	50.00	79.41	56.00	0.4510	0.5300		
	Other (108)	69.44	61.11	44.44	55.55	81.94	62.96	0.7060	0.5926		
All subjects (151)		68.21	58.94	37.77	53.33	81.13	61.32	0.6631	0.5733		

2018). The probability men get misdiagnosed for stroke is lower than women (Newman-Toker et al., 2014). To compare how clinicians and our model perform regarding this discrepancy, we report results on different gender groups.

- **Age.** The risk for stroke increases with age. According to national statistics, the majority of patients hospitalized for stroke are over 65 years old (Hall et al., 2012). This prior is not clearly shown in our dataset, partly because some older patients are having more serious conditions and are not enrolled in this study.
- **Ethnicity.** According to Trimble and Morgenstern (2008), the incidence of stroke in Hispanics is significantly higher than in Non-Hispanic whites. Hispanics are also believed to have a higher rate of stroke recurrence (Sheinart et al., 1998). Note that due to the relatively limited Hispanic participants in our current version of dataset, the comparison may not be indicative enough for the discrepancy.
- **Race.** African Americans have nearly twice as high risk of first stroke comparing to others (Virani et al., 2020) and the highest mortality rate (Centers for Disease Control and Prevention.). African Americans also receive less evidence-based care and have a higher risk of stroke recurrence (Schwamm et al., 2010). Another potential issue is concerned with the biases in current face-related computational models that are mainly trained on image/video samples from non-African-American participants.

Table 5 shows that the validations on most of the attribution groups result in a relatively stable AUC (variations are expected considering the relatively small number of samples). For the attribute of gender and ethnicity, the variation among different groups can be regarded as reasonable. The results on African American subjects raise some concern as the AUC falls to 0.451, indicating that the model trained on the complete dataset is not picking up the African American cases very well. We argue this is due to the larger imbalance of positive/negative

cases among African American groups compared to the complete dataset (34 stroke, 9 non-stroke). A further ablation study is conducted to train the framework on other cases and validate on African American cases and the result is shown in Table 6.

Table 6: Validation results for African American cases when training the framework on other cases.

Attr.	Accuracy (%)	Specificity (%)	Sensitivity (%)	AUC
African American (43)	65.90	11.11	80.00	0.5142

With a roughly 4:1 imbalance ratio, a random guess with prior will result in 80% sensitivity and 20% specificity. The above result indicates that while our dataset has been trying to capture diversity in patients, only 9 non-stroke patient cases may not be enough to fairly train and evaluate the proposed model. This is especially the case when performing the 5-fold cross-validation, where each testing set will only have at most two African American non-stroke cases. Every small error in such cases will result in a huge drop in the model performance on this specific attribute group. Future data collection will help to address this issue. Another potentially biased attribute group is age. Both the model and clinical impression have a rather large discrepancy in specificity between the two age groups, and cases younger than 65 years old are much higher in specificity. To further look into and attempt to understand this discrepancy, we first train on younger cases and validate on older cases, and then do the reverse. The results are shown in Table 7.

Table 7: Ablation study on age attribute. The first row is trained on younger cases (≤ 65 y/o) and tested on older cases (≥ 65 y/o), and the second row is trained on older cases and trained on younger cases.

Attr.	Accuracy (%)	Specificity (%)	Sensitivity (%)	AUC
≤ 65 y/o	88.06	66.67	97.83	0.9089
≥ 65 y/o	86.90	79.17	90.00	0.9080

The result is showing very good classification results, which partly indicates more homogeneity between the training and testing set. While age is a known factor for the risk of stroke, the homogeneity can be somewhat counter-intuitive. We infer this improvement in performance lays in that different patterns of a stroke may distribute evenly among cases in two different age groups in our dataset, and the effect shall be further examined when more data is incorporated.

6. Discussion

We analyze the running time of the proposed approach. The recording runs for a minute, the extraction of audio and generation of spectrograms takes an extra minute, and the video processing is completed in three minutes. The prediction with the deep models can be achieved within half a minute on a desktop with NVIDIA GTX 1070 GPU. Therefore, the evaluation process takes no more than six minutes per case. More importantly, the process is almost running at zero external cost and would be contactless, not harming the patients with equipment or by radiation. Considering a complete MRI scan will take more than an hour to perform, a specialized device to run, and hundreds of dollars charged, the proposed method is more ideal for performing both cost and time-efficient stroke assessments in an emergency setting.

We also expect that our proposed approach will be clinically relevant and can be deployed effectively on smartphones for fast and accurate assessment of stroke by ER doctors, telestroke neurologists, at-risk patients, or caregivers. If the approach is further optimized and deployed onto a smartphone, we can perform the spatiotemporal face frame proposal and speech audio processing on the phone. Cloud computing can be leveraged to perform the prediction in no more than a minute after the frames are compressed and uploaded. In such a case, the total time for one assessment should be within three to four minutes. Moreover, with minimal user education required, such a framework can allow for the patients' self-assessments even before the ambulance arrives. With different labeling of data, the pipeline is also valuable in the screening of other oral-facial neurological conditions.

Through our experiment, we noticed that the dataset we have been collecting for the pilot study purposes is still preliminary and small, especially for the evaluation of demographics. Also, with a limited number of cases available, the dataset could be insufficient to cover all possible patterns of stroke in facial motions and speech. The limitation also leads to the performance discrepancy on the African American cases and among age-related attribute groups. We're working towards a large-scale clinical trial (≈ 1000 cases) to evaluate the proposed method and further improve the robustness. When enough data is available, we would also pick a verified set of held-out test data to cover expected variations and use it as the public evaluation standard for this task.

We also noticed that when clinicians are performing stroke screening in the ER, they would consider race, ethnicity, and age as factors, and they may also refer to the patients' EHR for previous stroke records. Such information is missing from our

dataset. While we would like to find patterns directly from facial motions and speaking voices, these factors are also good to be adopted as auxiliary information that may guide the framework to project different probabilities of stroke for different demographics groups referring to the prior distributions.

We recognize other limitations of our work. First, the spatiotemporal facial frame proposal method is preliminary and is unable to eliminate all non-facial motions. This induces errors in the captured facial motion features. Also, the state-of-the-art 2D facial landmark tracking and pose estimation algorithms still induce considerable error in the pipeline. A plan is to collect 3D data instead of 2D so that we could achieve accurate alignment and reconstruction of subjects' faces. With accurate mesh representation of the subjects' facial motions, we could model the motions of different facial regions and correlate them to different areas of brain lesions. The representation could also help reduce color bias and naturally remove identity from subjects, which is promising. Second, the computational workload of the whole pipeline is still heavy for mobile deployment. In conditions with low network bandwidth, the transfer of collected data could be a serious bottleneck and hinder the efficiency of the screening process. Future work would need to address these issues and improve the framework for even better clinical performance.

7. Conclusion

In this work, we presented a novel multi-modal deep learning framework, *DeepStroke*, for on-site clinical detection of stroke in an ER setting. Our framework can perform accurate and efficient stroke screening based on the abnormalities in the patient's speech ability and facial muscular movements. We constructed a dual branch deep neural network for the classification of patient facial video frame sequences and speech audio as spectrograms to capture subtle stroke patterns from both modalities. Experiments on our collected clinical dataset with real, diverse, "in-the-wild" ER patients demonstrated that the proposed approach not only matches the ER physician, but outperforms clinicians in the ER in providing a binary clinical impression on the existence of a stroke, with a 6.60% higher sensitivity rate and 4.62% higher accuracy when specificity is aligned. Also, ablation studies validated the value of our multimodal lateral fusion method and adversarial training scheme, which collaboratively improve our proposed model from our prior work. The DSN has also been verified to be efficient and provide a screening result for the reference of clinicians in minutes.

Before a clinical deployment, we would continue to conduct the clinical trial, enlarge the dataset, improve the efficiency of the pipeline and develop the current method into a 3D mobile framework. Future efforts may also try to address the potential biases in the current model and apply the method to other neurological conditions.

References

- Akkus, Z., Galimzianova, A., Hoogi, A., Rubin, D.L., Erickson, B.J., 2017. Deep learning for brain MRI segmentation: state of the art and future directions. *Journal of digital imaging* 30, 449–459.

- Amodei, D., Ananthanarayanan, S., Anubhai, R., Bai, J., Battenberg, E., Case, C., Casper, J., Catanzaro, B., Cheng, Q., Chen, G., et al., 2016. Deep Speech 2: End-to-end speech recognition in English and Mandarin, in: Proceedings of the International Conference on Machine Learning, pp. 173–182.
- Anping, S., Guoliang, X., Xuehai, D., Jiabin, S., Gang, X., Wu, Z., 2017. Assessment for facial nerve paralysis based on facial asymmetry. *Australasian Physical & Engineering Sciences in Medicine* 40, 851–860.
- Bandini, A., Orlandi, S., Escalante, H.J., Giovannelli, F., Cincotta, M., Reyes-Garcia, C.A., Vanni, P., Zaccara, G., Manfredi, C., 2017. Analysis of facial expressions in Parkinson's disease through video-based automatic methods. *Journal of Neuroscience Methods* 281, 7–20. URL: <https://www.sciencedirect.com/science/article/pii/S0165027017300481>.
- Bandini, A., Orlandi, S., Giovannelli, F., Felici, A., Cincotta, M., Clemente, D., Vanni, P., Zaccara, G., Manfredi, C., 2016. Markerless analysis of articulatory movements in patients with Parkinson's disease. *Journal of Voice* 30, 766. e–766. e11.
- Banks, C.A., Bhama, P.K., Park, J., Hadlock, C.R., Hadlock, T.A., 2015. Clinician-graded electronic facial paralysis assessment: The eface. *Plastic and Reconstructive Surgery* 136, 223e–230e.
- Bevilacqua, V., D'Ambruoso, D., Mandolino, G., Suma, M., 2011. A new tool to support diagnosis of neurological disorders by means of facial expressions, in: Proceedings of the IEEE International Symposium on Medical Measurements and Applications, IEEE, pp. 544–549.
- Cai, J., Meng, Z., Khan, A.S., Li, Z., O'Reilly, J., Tong, Y., 2019. Identity-free facial expression recognition using conditional generative adversarial network. arXiv preprint arXiv:1903.08051 .
- Carreira, J., Zisserman, A., 2017. Quo vadis, action recognition? a new model and the kinetics dataset, in: Proceedings of the IEEE Conference on Computer Vision and Pattern Recognition, pp. 6299–6308.
- Centers for Disease Control and Prevention, . Underlying Cause of Death, 1999–2018. *CDC WONDER Online Database. Atlanta, GA: Centers for Disease Control and Prevention* [Online]. Available: <https://wonder.cdc.gov/ucd-icd10.html>. [Accessed 12-Mar-2021].
- Centers for Disease Control and Prevention, 2005. About Stroke. *CDC Stroke. Atlanta, GA: Centers for Disease Control and Prevention* [Online]. Available: <https://www.cdc.gov/stroke/about.htm>. [Accessed 12-Mar-2021].
- Centers for Disease Control and Prevention, 2020. Stroke Facts. *CDC Stroke. Atlanta, GA: Centers for Disease Control and Prevention* [Online]. Available: <https://www.cdc.gov/stroke/facts.htm>. [Accessed 12-Mar-2021].
- Colsch, R., Lindseth, G., 2018. Unique stroke symptoms in women: A review. *Journal of Neuroscience Nursing* 50, 336–342.
- Danelljan, M., Bhat, G., Shahbaz Khan, F., Felsberg, M., 2017. Eco: Efficient convolution operators for tracking, in: Proceedings of the IEEE Conference on Computer Vision and Pattern Recognition, pp. 6638–6646.
- Deng, J., Dong, W., Socher, R., Li, L., Kai Li, Li Fei-Fei, 2009. ImageNet: A large-scale hierarchical image database, in: Proceedings of the IEEE Conference on Computer Vision and Pattern Recognition, pp. 248–255. doi:10.1109/CVPR.2009.5206848.
- Dong, J., Lin, Y., an Liu, L., Ma, L., Wang, S., 2008. An approach to evaluation of degree of facial paralysis based on image processing and pattern recognition. *Journal of Information & Computational Science* 5, 639–646.
- Eitel, A., Springenberg, J.T., Spinello, L., Riedmiller, M., Burgard, W., 2015. Multimodal deep learning for robust RGB-D object recognition, in: Proceedings of the IEEE/RSJ International Conference on Intelligent Robots and Systems (IROS), pp. 681–687. doi:10.1109/IR0S.2015.7353446.
- Feichtenhofer, C., Fan, H., Malik, J., He, K., 2019. Slowfast networks for video recognition, in: Proceedings of the IEEE/CVF International Conference on Computer Vision, pp. 6202–6211.
- Flores-Mondragón, G., Paredes-Espinoza, M.A., Hernández-Campos, N.A., Sánchez-Chapul, L., Paniagua-Pérez, R., Martínez-Canseco, C., Renán-León, S., Araujo-Monsalvo, V.M., Perea-Paz, J.M., Flores-Jacinto, A., 2015. Facial anthropometry: A tool for quantitative evaluation in patients with peripheral facial paralysis. *Int.J.Sci.Eng.Res* 6, 1657–1660.
- Frey, M., Michaelidou, M., Tzou, C.H., Pona, I., Mittlböck, M., Gerber, H., Stüssi, E., 2008. Three-dimensional video analysis of the paralyzed face reanimated by cross-face nerve grafting and free gracilis muscle transplantation: Quantification of the functional outcome. *Plastic and Reconstructive Surgery* 122, 1709–1722.
- Giles, E., Patterson, K., Hodges, J.R., 1996. Performance on the Boston Cookie Theft picture description task in patients with early dementia of the Alzheimer's type: Missing information. *Aphasiology* 10, 395–408.
- Goodfellow, I.J., Pouget-Abadie, J., Mirza, M., Xu, B., Warde-Farley, D., Ozair, S., Courville, A., Bengio, Y., 2014. Generative adversarial networks. arXiv preprint arXiv:1406.2661 .
- Green, R.D., Guan, L., 2004. Quantifying and recognizing human movement patterns from monocular video images-part ii: Applications to biometrics. *IEEE Transactions on Circuits and Systems for Video Technology* 14, 191–198.
- Greene, J.J., Guarin, D.L., Tavares, J., Fortier, E., Robinson, M., Dusseldorp, J., Quatela, O., Jowett, N., Hadlock, T., 2019. The spectrum of facial palsy: The MEEI facial palsy photo and video standard set. *The Laryngoscope* URL: <https://www.ncbi.nlm.nih.gov/pubmed/31021433>.
- Guo, Z., Shen, M., Duan, L., Zhou, Y., Xiang, J., Ding, H., Chen, S., Deussen, O., Dan, G., 2017. Deep assessment process: Objective assessment process for unilateral peripheral facial paralysis via deep convolutional neural network, in: Proceedings of the 2017 IEEE International Symposium on Biomedical Imaging, pp. 135–138.
- Hakata, M., Seo, M., Chen, Y., Matsushiro, N., 2013. Facial paralysis modeling based on image morphing, in: Proceedings of the 6th International Conference on Biomedical Engineering and Informatics, pp. 806–810. doi:10.1109/BMEI.2013.6747051.
- Hall, M.J., Levant, S., DeFrances, C.J., 2012. Hospitalization for stroke in US hospitals, 1989-2009. 56, US Department of Health and Human Services, Centers for Disease Control and . . .
- Hamm, J., Kohler, C.G., Gur, R.C., Verma, R., 2011. Automated Facial Action Coding System for dynamic analysis of facial expressions in neuropsychiatric disorders. *Journal of Neuroscience Methods* 200, 237–256. URL: <https://www.sciencedirect.com/science/article/pii/S016502701100358X>.
- Hannun, A., Case, C., Casper, J., Catanzaro, B., Diamos, G., Elsen, E., Prenger, R., Satheesh, S., Sengupta, S., Coates, A., et al., 2014. Deep Speech: Scaling up end-to-end speech recognition. arXiv preprint arXiv:1412.5567 .
- Harbison, J., Hossain, O., Jenkinson, D., Davis, J., Louw, S.J., Ford, G.A., 2003. Diagnostic accuracy of stroke referrals from primary care, emergency room physicians, and ambulance staff using the face arm speech test. *Stroke* 34, 71–76.
- He, S., Soraghan, J.J., O'Reilly, B.F., 2007. Automatic motion feature extraction with application to quantitative assessment of facial paralysis, in: Proceedings of the IEEE International Conference on Acoustics, Speech and Signal Processing, p. 444.
- He, S., Soraghan, J.J., O'Reilly, B.F., 2008. Supervised local linear embedding (SLLLE) for facial paralysis image sequence analysis, in: Proceedings of the IEEE International Conference on Multimedia and Expo, IEEE, pp. 49–52.
- House, J.W., Brackmann, D.E., 1985. Facial nerve grading system. *Otolaryngology-Head and Neck Surgery* 93, 146–147. URL: <https://journals.sagepub.com/doi/full/10.1177/019459988509300202>.
- Hsu, G.J., Huang, W., Kang, J., 2018. Hierarchical network for facial palsy detection, in: Proceedings of the IEEE/CVF Conference on Computer Vision and Pattern Recognition Workshops (CVPRW), pp. 693–6936. doi:10.1109/CVPRW.2018.00100.
- Huang, S.C., Pareek, A., Seyyedi, S., Banerjee, I., Lungren, M.P., 2020. Fusion of medical imaging and electronic health records using deep learning: A systematic review and implementation guidelines. *NPJ digital medicine* 3, 1–9.
- Johnson, W., Onuma, O., Owolabi, M., Sachdev, S., 2016. Stroke: A global response is needed. *Bulletin of the World Health Organization* 94, 634.
- Kahou, S.E., Bouthillier, X., Lamblin, P., Gulcehre, C., Michalski, V., Konda, K., Jean, S., Froumenty, P., Dauphin, Y., Boulanger-Lewandowski, N., et al., 2016. Emonets: Multimodal deep learning approaches for emotion recognition in video. *Journal on Multimodal User Interfaces* 10, 99–111.
- Kihara, Y., Duan, G., Nishida, T., Matsushiro, N., Chen, Y.W., 2011. A dynamic facial expression database for quantitative analysis of facial paralysis, in: Proceedings of the 6th International Conference on Computer Sciences and Convergence Information Technology (ICCIT), IEEE, pp. 949–952.
- King, D.E., 2009. Dlib-ml: A machine learning toolkit. *Journal of Machine Learning Research* 10, 1755–1758.
- Kothari, R.U., Pancioli, A., Liu, T., Brott, T., Broderick, J., 1999. Cincinnati prehospital stroke scale: Reproducibility and validity. *Annals of Emergency Medicine* 33, 373–378.
- Lee, H.Y., Tseng, H.Y., Huang, J.B., Singh, M., Yang, M.H., 2018. Diverse image-to-image translation via disentangled representations, in: Proceedings of the European conference on computer vision (ECCV), pp. 35–51.

- Leira, E.C., Kaskie, B., Froehler, M.T., Adams Jr, H.P., 2013. The growing shortage of vascular neurologists in the era of health reform: Planning is brain! *Stroke* 44, 822–827.
- Li, Y., Shen, L., 2018. Deep learning based multimodal brain tumor diagnosis, in: Crimi, A., Bakas, S., Kuijf, H., Menze, B., Reyes, M. (Eds.), *Brainlesion: Glioma, Multiple Sclerosis, Stroke and Traumatic Brain Injuries*, Springer International Publishing, Cham. pp. 149–158.
- Liang, M., Li, Z., Chen, T., Zeng, J., 2015. Integrative data analysis of multiplatform cancer data with a multimodal deep learning approach. *IEEE/ACM Transactions on Computational Biology and Bioinformatics* 12, 928–937. doi:10.1109/TCBB.2014.2377729.
- Lin, M., Chen, Q., Yan, S., 2013. Network in network. arXiv preprint arXiv:1312.4400.
- Liu, Y., Wei, F., Shao, J., Sheng, L., Yan, J., Wang, X., 2018. Exploring disentangled feature representation beyond face identification, in: *Proceedings of the IEEE Conference on Computer Vision and Pattern Recognition*, pp. 2080–2089.
- Lu, B., Chen, J.C., Chellappa, R., 2019. Unsupervised domain-specific deblurring via disentangled representations, in: *Proceedings of the IEEE Conference on Computer Vision and Pattern Recognition*, pp. 10225–10234.
- Lucey, P., Cohn, J.F., Kanade, T., Saragih, J., Ambadar, Z., Matthews, I., 2010. The extended Cohn-Kanade dataset (ck+): A complete dataset for action unit and emotion-specified expression, in: *Proceedings of the IEEE Computer Society Conference on Computer Vision and Pattern Recognition - Workshops*, pp. 94–101. doi:10.1109/CVPRW.2010.5543262.
- Mao, X., Li, Q., Xie, H., Lau, R.Y., Wang, Z., Paul Smolley, S., 2017. Least squares generative adversarial networks, in: *Proceedings of the IEEE International Conference on Computer Vision*, pp. 2794–2802.
- Menegotto, A.B., Lopes Becker, C.D., Cazella, S.C., 2020. Computer-aided hepatocarcinoma diagnosis using multimodal deep learning, in: Novais, P., Lloret, J., Chamoso, P., Carneiro, D., Navarro, E., Omatu, S. (Eds.), *Ambient Intelligence - Software and Applications - 10th International Symposium on Ambient Intelligence*, Springer International Publishing, Cham. pp. 3–10.
- Meng, Z., Liu, P., Cai, J., Han, S., Tong, Y., 2017. Identity-aware convolutional neural network for facial expression recognition, in: *2017 12th IEEE International Conference on Automatic Face Gesture Recognition (FG 2017)*, pp. 558–565. doi:10.1109/FG.2017.140.
- Newman-Toker, D.E., Moy, E., Valente, E., Coffey, R., Hines, A.L., 2014. Missed diagnosis of stroke in the emergency department: a cross-sectional analysis of a large population-based sample. *Diagnosis* 1, 155–166.
- Ngiam, J., Khosla, A., Kim, M., Nam, J., Lee, H., Ng, A.Y., 2011. Multimodal deep learning, in: *Proceedings of the International Conference on Machine Learning*, pp. 689–696. URL: https://icml.cc/2011/papers/399_icmlpaper.pdf.
- Ngo, T.H., Seo, M., Matsushiro, N., Xiong, W., Chen, Y.W., 2016. Quantitative analysis of facial paralysis based on limited-orientation modified circular gabor filters, in: *Proceedings of the 23rd International Conference on Pattern Recognition (ICPR)*, IEEE. pp. 349–354.
- NIH, 2003. NIH Stroke Scale. *National Institutes of Health*. [Online]. Available: <https://www.stroke.nih.gov/resources/scale.htm>. [Accessed 17-Jan-2021].
- Perveen, N., 2019. Facial paralysis dataset. URL: <https://dx.doi.org/10.21227/6dsz-7d76>, doi:10.21227/6dsz-7d76.
- Radford, A., Metz, L., Chintala, S., 2015. Unsupervised representation learning with deep convolutional generative adversarial networks. arXiv preprint arXiv:1511.06434.
- Rafay, M.F., Pontigon, A.M., Chiang, J., Adams, M., Jarvis, D.A., Silver, F., MacGregor, D., deVeber, G.A., 2009. Delay to diagnosis in acute pediatric arterial ischemic stroke. *Stroke* 40, 58–64.
- Rogers, C.R., Schmidt, K.L., VanSwearingen, J.M., Cohn, J.F., Wachtman, G.S., Manders, E.K., Deleyiannis, F.W.B., 2007. Automated facial image analysis: Detecting improvement in abnormal facial movement after treatment with botulinum toxin A. *Annals of Plastic Surgery* 58, 39–47.
- Ross, B.G., Fradet, G., Nedzelski, J.M., 1996. Development of a sensitive clinical facial grading system. *Otolaryngology—Head and Neck Surgery* 114, 380–386.
- Schwamm, L.H., Reeves, M.J., Pan, W., Smith, E.E., Frankel, M.R., Olson, D., Zhao, X., Peterson, E., Fonarow, G.C., 2010. Race/ethnicity, quality of care, and outcomes in ischemic stroke. *Circulation* 121, 1492.
- Sheinart, K., Tuhim, S., Horowitz, D., Weinberger, J., Goldman, M., Godbold, J., 1998. Stroke recurrence is more frequent in Blacks and Hispanics. *Neuroepidemiology* 17, 188–198.
- Song, A., Wu, Z., Ding, X., Hu, Q., Di, X., 2018. Neurologist standard classification of facial nerve paralysis with deep neural networks. *Future Internet* 10, 111.
- Stevens, S.S., Volkman, J., Newman, E.B., 1937. A scale for the measurement of the psychological magnitude pitch. *The Journal of the Acoustical Society of America* 8, 185–190.
- Storey, G., Jiang, R., 2018. Face symmetry analysis using a unified multi-task CNN for medical applications, in: *Proceedings of SAI Intelligent Systems Conference*, Springer. pp. 451–463.
- Szczapa, B., Daoudi, M., Kacem, A., Guerreschi, P., Gebert, L., Alvarez-Paiva, J.C., 2019. 2D landmark-based facial asymmetry assessment in the clinical case of facial paralysis, in: *Proceedings of the IEEE International Conference on Automatic Face & Gesture Recognition*, IEEE. pp. 1–5.
- Thevenot, J., López, M.B., Hadid, A., 2017. A survey on computer vision for assistive medical diagnosis from faces. *IEEE Journal of Biomedical and Health Informatics* 22, 1497–1511.
- Tran, L., Yin, X., Liu, X., 2017. Disentangled representation learning GAN for pose-invariant face recognition, in: *Proceedings of the IEEE conference on computer vision and pattern recognition*, pp. 1415–1424.
- Trimble, B., Morgenstern, L.B., 2008. Stroke in minorities. *Neurologic clinics* 26, 1177–1190.
- Virani, S.S., Alonso, A., Benjamin, E.J., Bittencourt, M.S., Callaway, C.W., Carson, A.P., Chamberlain, A.M., Chang, A.R., Cheng, S., Delling, F.N., et al., 2020. Heart disease and stroke statistics—2020 update: A report from the American Heart Association. *Circulation* 141, e139–e596.
- Vásquez-Correa, J.C., Arias-Vergara, T., Orozco-Arroyave, J.R., Eskofier, B., Klucken, J., Nöth, E., 2019. Multimodal assessment of Parkinson's disease: A deep learning approach. *IEEE Journal of Biomedical and Health Informatics* 23, 1618–1630. doi:10.1109/JBHI.2018.2866873.
- Wang, C., Wang, S., Liang, G., 2019. Identity- and pose-robust facial expression recognition through adversarial feature learning, in: *Proceedings of the 27th ACM International Conference on Multimedia*, Association for Computing Machinery, New York, NY, USA. p. 238–246.
- Wang, T., Dong, J., Sun, X., Zhang, S., Wang, S., 2014. Automatic recognition of facial movement for paralyzed face. *Bio-medical materials and engineering* 24, 2751–2760.
- Wang, T., Zhang, S., Dong, J., Liu, L., Yu, H., 2016. Automatic evaluation of the degree of facial nerve paralysis. *Multimedia Tools and Applications* 75, 11893–11908.
- Xiao, F., Lee, Y.J., Grauman, K., Malik, J., Feichtenhofer, C., 2020. Audiovisual slowfast networks for video recognition. arXiv preprint arXiv:2001.08740.
- Xu, T., Zhang, H., Huang, X., Zhang, S., Metaxas, D.N., 2016. Multimodal deep learning for cervical dysplasia diagnosis, in: *Proceedings of the International Conference on Medical Image Computing and Computer-Assisted Intervention*, Springer. pp. 115–123.
- Xue, Y., Xu, T., Zhang, H., Long, L.R., Huang, X., 2018. Segan: Adversarial network with multi-scale l1 loss for medical image segmentation. *Neuroinformatics* 16, 383–392.
- Yao, J., Xu, Z., Huang, X., Huang, J., 2018. An efficient algorithm for dynamic mri using low-rank and total variation regularizations. *Medical Image Analysis* 44, 14–27. URL: <https://www.sciencedirect.com/science/article/pii/S1361841517301585>, doi:https://doi.org/10.1016/j.media.2017.11.003.
- Yu, M., Cai, T., Huang, X., Wong, K., Volpi, J., Wang, J.Z., Wong, S.T.C., 2020. Toward rapid stroke diagnosis with multimodal deep learning, in: *Proceedings of the Medical Image Computing and Computer Assisted Intervention*, Springer International Publishing, Cham. pp. 616–626.
- Zhang, Z., Tran, L., Yin, X., Atoum, Y., Liu, X., Wan, J., Wang, N., 2019. Gait recognition via disentangled representation learning, in: *Proceedings of the IEEE Conference on Computer Vision and Pattern Recognition*, pp. 4710–4719.
- Zhuang, Y., Uribe, O., McDonald, M., Lin, I., Arteaga, D., Dalrymple, W., Worrall, B., Southerland, A., Rohde, G., 2018. Pathological facial weakness detection using computational image analysis, in: *Proceedings of the IEEE 15th International Symposium on Biomedical Imaging*, IEEE. pp. 261–264.
- Zhuang, Y., Uribe, O., McDonald, M., Yin, X., Parikh, D., Southerland, A., Rohde, G., 2019. F-DIT-V: An automated video classification tool for facial weakness detection, in: *Proceedings of the 2019 IEEE EMBS International Conference on Biomedical & Health Informatics (BHI)*, IEEE. pp. 1–4.